Regular and chaotic oscillations of friction force

A Stefański[1], **J Wojewoda**[1], **M Wiercigroch**[2*], and **T Kapitaniak**[1]
[1]Division of Dynamics, Technical University of Łódź, Łódź, Poland
[2]Centre for Applied Dynamics Research, University of Aberdeen, King's College, Aberdeen, UK

The manuscript was received on 15 November 2005 and was accepted after revision for publication on 9 December 2005.

DOI: 10.1243/09544062C09305

Abstract: In this paper, several friction features and models are discussed in the context of the dynamical nature of friction force observed during experiments. On the basis of experimental and theoretical analysis, the authors show that such behaviour can be considered as a certain representation of the system dynamics. According to this approach, a classification of friction models with respect to their sensitivity on the system motion character is introduced. Next, the results of experimental research are reported. Friction characteristics reconstructed experimentally for various types of the system response, i.e. periodic, quasi-periodic, and chaotic, are demonstrated. Finally, these results are compared with numerical simulations using the proposed friction model.

Keywords: dry friction, dynamics, chaos, experimental studies

1 INTRODUCTION

The phenomenon of friction appears in many, if not all, mechanical systems, e.g. wheels, brakes, valves, cylinders, bearings, transmissions, etc. Particularly interesting seems to be the problem of dry friction, which is often a reason of self-excited vibrations, commonly met in engineering practice. Usually, this is an unnecessary effect and a most unwanted one. Such self-excited vibrations cause an early wear of the contacting parts of machines and, if not under control, could have much more dangerous consequences. For many years, the topic of dry friction has been a subject of active research with many attempts to identify the causes of its behaviour such as the squeal of car brakes, extensive wear of cutting tools and others. The problems with dry friction occur also in design and utilizing of rail-vehicles and machines.

From the mathematical point of view, dry friction problems are also cumbersome as their inclusion implicates appearance of the discontinuous differential equations, where the character of this discontinuity depends upon the friction character adopted. In general, there are many different types of dry friction models and it is crucial to appropriately choose one, which best suits the modelled problem. For example, if one considers dynamics of the system where the relative velocity practically remains constant, there is no need for sophisticated dry friction models and even the simplest one described by the Coulomb law will suffice. However, in many cases the variation of the relative velocity is large and often the velocity changes its sign. In such situations, the chosen model must account for the transition from static to dynamic friction and should provide a means of guiding the system through zero relative velocity. These types of friction models should be able to predict both phases of stick with a higher friction coefficient and slip where this coefficient is smaller. These are the reasons why systems with dry friction possess many different types of dynamical behaviour, such as periodical, non-periodic, chaotic, and sometimes even static responses [**1**–**23**].

However, from a viewpoint of the experiment, even the most advanced approaches provide a realistic approximation of friction force only for regular response of the system. In case of irregular motion the friction characteristics generated from experiments often have much more complicated forms than those predicted by most of the existing friction models. This fact cannot be explained through

*Corresponding author: Centre for Applied Dynamics Research, University of Aberdeen, King's College, Aberdeen AB24 8UE, UK. email: m.wiercigroch@eng.abdn.ac.uk

measurement errors. During our earlier research, the authors have also observed that dynamical behaviour of friction force can be dependent on the system dynamics [**14**–**16**, **22**, **23**]. The main purpose of this paper is to develop a mathematical explanation of dynamic responses obtained from experimental studies.

The paper is organized as follows. Section 2 contains a short review of several examples of existing friction models (static and dynamic) and ideas concerning the nature of friction force. A description of the experimental rig and its mathematical model is given in section 3 together with the experimental results. In section 4, the authors present their model of dry friction and its comparison with experimental results. The last section draws some conclusions.

2 FRICTION PHENOMENA AND MODELLING

Friction force is a reaction in the tangential direction between a pair of contacting surfaces. Dry friction phenomenon can be treated as the result of various factors, i.e. physical properties of the material of frictional surfaces, its geometry and topology, relative velocity, and displacement of the bodies in contact. Dynamical behaviour of friction force has been actively researched since Coulomb's hypothesis. Some newer experiments (from the beginning of the 20th century) show non-linear dependence on the contact velocity rather than the constant one, e.g. see [**12**, **17**]. That was why most efforts were directed to build non-linear friction models and to determine differences in maximal values of the static and dynamic friction forces. These experiments have often been performed for stationary conditions, e.g. constant velocity. The friction force as a function of velocity for constant velocity motion is called the Stribeck curve [**17**]. Stribeck's work has shown a non-linear transition from stick to slip. Therefore, the dip in friction force (see Fig. 1(a)) observed at low values of the relative velocity is called the Stribeck effect. An interesting problem of stick–slip transition is a break-away force [**12**], i.e. the force required to stop sticking and initiate the motion. Experimental study on the nature of static friction and break-away force led to the conclusion that the magnitude of this force depends on the rate of increase of the friction force during stick [**7**]. Hence, varying level of break-away force can be identified as a function of a dwell time, i.e. time at zero velocity (Fig. 1(b)).

Another friction feature, which can appear during the switch between stick and slide phases is the spring-like behaviour of friction force before the actual sliding. This microscopic motion phenomenon,

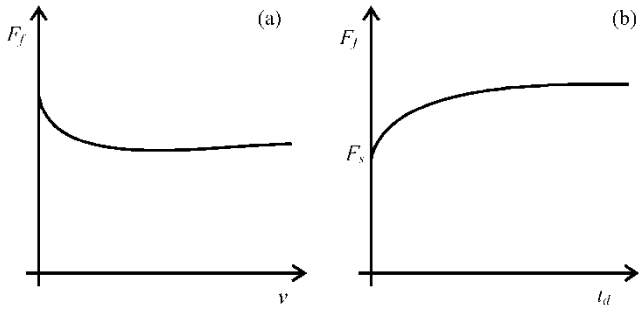

Fig. 1 Non-linear friction force F_f represented as: Stribeck curve, v, velocity of the relative motion (a) and break-away force F_S a function of a dwell time t_d (b)

also called pre-sliding displacement effect, is caused by tangential stiffness between bodies in contact (compliant contact) [**5**, **8**, **24**]. Such contact compliance may arise from elastic deformation near the contact point or in the surrounding structure. Pre-sliding motion is represented by a narrow hysteresis (in the horizontal direction) around the zero relative velocity (Fig. 2(a)) and the slope in the vertical direction on the friction force versus displacement diagram (Fig. 2(b)).

Other hysteresis effects can appear during oscillations with macroscopic sliding, i.e. periodic, relatively large-scale motion with pure sliding. Such phenomenon has been reported for the first time for experiments with a periodic relative velocity of unidirectional motion, see [**6**]. Friction-relative velocity relation obtained experimentally appeared as in Fig. 3(a). Hysteresis was observed as the velocity varied. The size of the loop increased as the velocity variations become faster [**9**]. The friction force is lower for decreasing velocities than for increasing velocities. Such hysteresis effect is explained by the existence of frictional memory caused by lag in the friction force. Similar hysteretic character of friction force can be also observed during regressive (two-way) oscillations with macroscopic sliding. Some

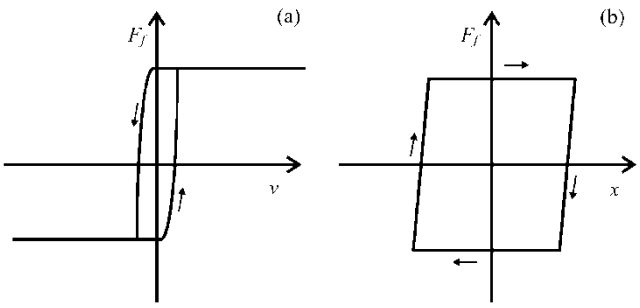

Fig. 2 Coulomb friction with a compliant contact

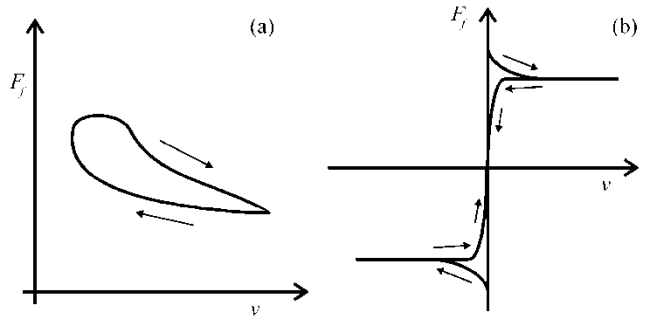

Fig. 3 Frictional memory (a) and non-reversible friction characteristic (b)

experimental and analytical studies confirm an existence of different slopes of friction force for the acceleration and deceleration phases [**1**, **2**] as shown in Fig. 3(b). This feature of friction is called non-reversibility of friction force [**11**, **20**, **21**].

On the basis of experimental investigations and analytical study, reported briefly earlier, some researchers have developed various friction models. A practical engineering approach, indebted to Coulomb simplifies the friction force to a constant value being opposite to the relative velocity of the contacting bodies

$$F_f = Nf_C \ \mathrm{sgn}(v) \tag{1}$$

where F_f is a friction force, N, the normal load, f_C, the coefficient of Coulomb friction, and v the relative velocity. Such a force takes two values with equal size amplitude but opposite in sign [**25**]. However, this classical friction model does not explain all dynamical behaviour and phenomena observed in mechanical systems with friction. For example, mathematical model of self-excited vibrations, induced by dry friction requires, non-zero slope of friction characteristic in order to initialize such kind of oscillations [**26**].

Non-linear friction characteristics, including e.g. the Stribeck effect, are better approximations of an actual character of friction. An example of a geometrically non-linear approach to friction force is the Popp–Stelter model [**10**]

$$F_f = N\left(\frac{f_S - f_C}{1 + \eta_1|v|} + f_C + \eta_2 v^2\right)\mathrm{sgn}(v) \tag{2}$$

where f_S is coefficient of static friction and η_1, η_2 are constants. Application of such a model in analysis enables us to explain the phenomena self-excited vibrations in mechanical systems with friction.

However, modelling of the hysteretic effects described previously connected with contact compliance or frictional memory requires even more sophisticated friction models. A simple approach to modelling the hysteretic behaviour of friction force has been proposed by Powell and Wiercigroch [**11**] and Wiercigroch [**21**]. Their idea is based on non-reversible friction characteristic, i.e. two different slopes of friction force depending on the sign of relative acceleration (Fig. 3(b)). Such non-reversible friction characteristic is defined by the following exponential friction relative velocity function

$$\begin{aligned} f_u(v) &= f_C\left[1 + \frac{f_S - f_C}{f_C}\exp\left(-a|v|\right)\right]\mathrm{sgn}(v), \\ &\quad \text{when} \quad \mathrm{sgn}\left(\frac{dv}{dt}\right) > 0 \\ f_l(v) &= f_C[1 - \exp\left(-b|v|\right)]\mathrm{sgn}(v), \\ &\quad \text{when} \quad \mathrm{sgn}\left(\frac{dv}{dt}\right) < 0 \end{aligned} \tag{3}$$

where $f_u(v)$, $f_l(v)$ are upper and lower parts of the characteristic for regions of increasing and decreasing relative velocity, respectively, a and b are constants that adjust the slopes of the characteristics. It results from equation (3) that in the case of non-reversible friction in the transition from stick to slip shows a decrease of the friction force, as assumed in the Stribeck model. However, during transition from slip to stick, the friction force does not reach the static value as in the case of reversible characteristics (e.g. model given by equation (2)), but decreases suddenly from the Coulomb value to zero.

Another known approach, which characterizes hysteretic behaviour of friction force is the Armstrong one [**27**], also called the seven parameters model. It is even more complicated than non-reversible friction characteristic because it actually consists of two separate models: one for stick phase and one for sliding. When the sticking friction is described by the linear spring model

$$F_f(x) = \beta x \tag{4a}$$

where β is a contact stiffness, in order to account for pre-sliding displacement. During sliding, the friction is modelled as Coulomb and viscous damping (F_v) with Stribeck effect and frictional memory

$$F_f(v, t) = \left[F_C + F_v|v| + F_S(\gamma, t_d)\frac{1}{1 + (v(t-\tau)/v_S)^2}\right] \times \mathrm{sgn}(v) \tag{4b}$$

where F_C is the Coulomb friction value, $F_S(\gamma, t_d)$ describes the varying friction level at break-away which depends on empirical parameter γ, and t_d

the dwell time, τ the time delay introducing to model a hysteretic effect of frictional memory and v_S is Stribeck velocity. As the model is defined by two separate equations, some mechanism must govern the switching between them.

All friction characteristics described earlier are classified as static models in contrast to dynamic friction models. The difference between them consists in the inclusion of frictional memory. For static friction models this frictional memory is omitted (equations (1) and (2)), modelled as non-reversibility (equation (3)), or described with frictional lag (equation (4b)). An alternative approach are dynamic friction models where memory behaviour is described with additional dynamics between velocity and the friction force. The main idea of such friction description is to introduce state variables (or internal states) that determine the level of friction apart from velocity. Time evolution of state variables is given by differential equation. The first approach that can be classified as dynamic friction model has been proposed by Dahl [**28**]. The base for the Dahl model is the stress–strain curve known from classical solid mechanics [**29**]

$$\frac{\mathrm{d}F_\mathrm{f}}{\mathrm{d}x} = \sigma\left(1 - \frac{F_\mathrm{f}}{F_\mathrm{C}}\operatorname{sgn}(v)\right)^{\alpha} \tag{5}$$

where σ is the stiffness coefficient and α determines the shape of stress–strain curve. The time dependence of the friction force in Dahl model (for $\alpha = 1$) can be obtained in the following way

$$\frac{\mathrm{d}F_\mathrm{f}}{\mathrm{d}t} = \frac{\mathrm{d}F_\mathrm{f}}{\mathrm{d}x}\frac{\mathrm{d}x}{\mathrm{d}t} = \frac{\mathrm{d}F_\mathrm{f}}{\mathrm{d}x}v = \sigma\left(v - \frac{F_\mathrm{f}}{F_\mathrm{C}}|v|\right) \tag{6}$$

Introducing $F_\mathrm{f} = \sigma z$, the model can be written as

$$\begin{aligned} \frac{\mathrm{d}z}{\mathrm{d}t} &= v - \frac{\sigma|v|}{F_\mathrm{C}}z \\ F_\mathrm{f} &= \sigma z \end{aligned} \tag{7}$$

where z is the internal state variable. Equation (7) exemplify a dynamic generalization of classical Coulomb friction. However, this approach does not model the Stribeck effect and static friction. These are the main motivation for further extensions of the Dahl model.

Recently, several more developed models, these include other observed friction properties, have been proposed [**4**, **30**, **31**]. An example of such approach is the LuGre model, which is related to the bristle interpretation of friction [**31**]. The model is described as follows

$$\begin{aligned} \frac{\mathrm{d}z}{\mathrm{d}t} &= v - \sigma_0\frac{|v|}{g(v)}z \\ F_\mathrm{f} &= \sigma_0 z + \sigma_1\frac{\mathrm{d}z}{\mathrm{d}t} + cv \end{aligned} \tag{8}$$

Here, the internal state variable z denotes the average bristle deflection, coefficients σ_0 and σ_1 determine the bristle stiffness and the bristle damping, respectively, cv the viscous friction and the function

$$g(v) = F_\mathrm{C} + (F_\mathrm{S} - F_\mathrm{C})\exp\left(-\left(\frac{v}{v_\mathrm{S}}\right)^2\right) \tag{9}$$

models the Stribeck effect. An advantage of the LuGre model is its rich dynamic behaviour giving possibilities of numerical modelling of observed friction phenomena such as stick–slip transition, varying break-away force, frictional memory and hysteretic behaviour, and Stribeck effect.

The brief review of friction models presented in this section concentrates on their dynamic characteristics, which can be used to classify these models. The friction characteristics can be divided into two groups, namely:

(a) independent of the system dynamics (e.g. equations (1) to (3));
(b) sensitive on a character of motion of the system (e.g. equations (4a); (4b) and equations (8), (9)).

Sensitivity of more developed models on the system dynamics is first and foremost caused by frictional memory and also by varying level of break-away force. In the case of steady-state motion, these factors have no influence on the friction force and it can be approximated precisely with classical Coulomb or Stribeck models. Even for simple periodic motion no significant differences between friction models from both groups can be observed. Periodic motion of the system results in the appearance of a hysteresis loop on friction characteristic because of the presence of frictional memory (lag) in the models from the second group, but the level of break-away force is the same in each cycle of motion because of the constant dwell time. However, similar hysteresis effect is modelled by non-reversible friction characteristic (equation (3)) from the first group. Significant difference between both groups of friction models can appear if motion of the system is multi-periodic or quasi-periodic, and in particular, if it is irregular motion of chaotic or stochastic character.

Irregular dynamics of the systems including frictional memory generates friction characteristics

consisted of many (or even infinitely many) hysteresis loops of different size. Also the break-away force possesses different values after each cycle because of varying dwell time. Hence, during irregular motion, the friction characteristics reconstructed on the basis of models from the second group take a form of some region in friction force versus relative velocity diagram. This is the reason, that such friction models are identified as sensitive (on the motion character). As a result of such sensitivity, the authors can observe a 'mapping effect' during the analysis of dry friction oscillators, i.e. friction characteristic is a reflection of the system attractor. In static friction models from the first group, the friction force is defined as a function of relative velocity according to the same formula for steady-state, regular, and irregular motion. Therefore, they are termed insensitive (on the motion character). In the next section, experimental verification of sensitive nature of friction force and the 'mapping effect' is presented.

During our earlier research [**15**, **16**, **22**], the authors have observed a kind of similarity between the type of the attractor of dynamical system with friction and dynamical behaviour of friction force. A friction model meeting these observations is also proposed [**15**]. This model was formulated on the basis of a symmetrical non-reversible friction characteristic and it is described by the following formula

$$f(v) = f_C\left[1 + \frac{f_S - f_C}{f_C}\exp\left(-\frac{a_1|v|}{|\mathrm{d}v/\mathrm{d}t| + a_2}\right)\mathrm{sgn}\left(\frac{\mathrm{d}v}{\mathrm{d}t}v\right)\right] \times \mathrm{sgn}(v) \tag{10}$$

where a_1 (1/s) and a_2 (m/s^2) are constants. A novelty of our approach is in the introduction of the current value of relative acceleration to the mathematical description of friction phenomenon, which allows us to model hysteretic frictional memory effect. Let us pay an attention, that the appearance of acceleration in friction model can also result from the seven parameters model (equations (4a), (4b)) because of the presence of time delay τ. Thus, our model (equation (10)) can be classified as static and sensitive on motion character, but unfortunately it does not model static friction. In section 4, a development of this approach is presented.

3 EXPERIMENTAL STUDIES

3.1 Experimental rig

The experimental oscillator designed by Wiercigroch *et al.* [**20**], shown in Fig. 4, comprises a block mass that oscillated along two guiding posts being supported with two coil springs, with a second mass

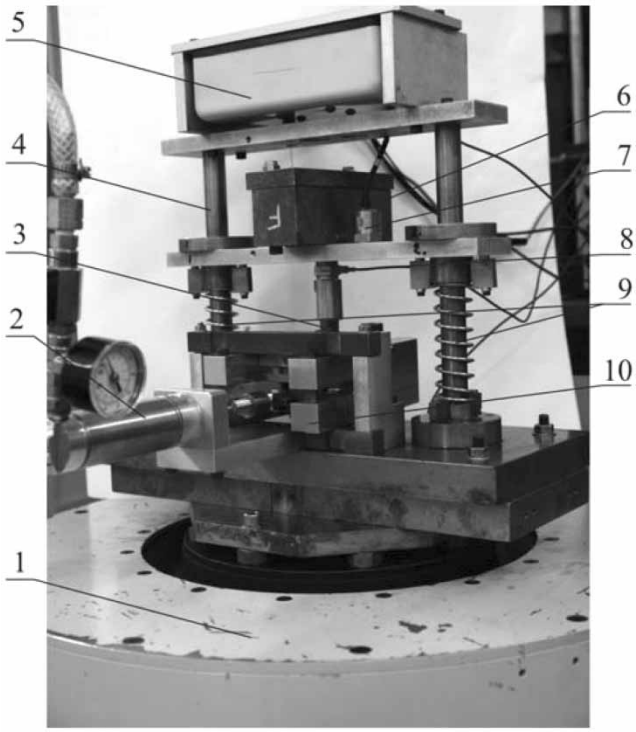

Fig. 4 General view of the experimental rig [**20**]: 1, shaker; 2, air pressure actuator with gauge; 3, friction tongue; 4, guiding post; 5, case of the LVT and LVDT transducers; 6, main mass; 7, accelerometer; 8, force transducer; 9, coil springs; 10, clamping mechanism

consisting of a vertical plate (tongue) introducing dry friction to the system. This plate can be in contact with two pads connected through a clamping mechanism to the base. A pneumatic actuator under constant air pressure supplies constant level of force acting on the clamping mechanism which presses both pads against the tongue. The design allows self-fitting of the friction elements to two swivel blocks housing the friction plates mounted in their slots using ball links. This helps to compensate for any misalignment of clamping even during oscillations. Different levels of clamping forces allowed for various normal pressure applied to friction pads and in consequence different amount of friction is induced. A friction mechanism providing the frictional force comprises a steel plate (tongue) and an adjustable pressure clamping mechanism with changeable frictional pads. The tongue is a vertically positioned steel plate mounted to a force transducer (FT) connected to the vibrating mass. The FT signal was taken from the FT but for an accurate evaluation of pure friction force, its necessary to subtract inertia force generated by the tongue itself. For measuring the relative velocity of the oscillating mass, a linear velocity transducer was used.

Different friction pad materials such as Teflon, aluminium, brass, and steel against steel tongue were used to test the dynamic responses in a wide range of parameters. The Teflon pads worked best in the device. As the variety of friction materials have different friction properties the clamping force needs to be varied in a wide range. Air pressure control provides for such flexibility, and does not allow for sticking between friction elements during motion (excluding extreme cases when air pressure was at extremely high level).

Slots were machined on to the two clamping faces of the tongue in order to remove debris generated during experiments. It is worth pointing out that only brass pads generated a large amount of debris. The rig was mounted on a shaker that provided the system with the necessary excitation. Sensing devices including accelerometers, velocity, displacement, and FTs were used to accurately monitor the state of the system. A computer data acquisition system and off-line data processing software were used to support in-depth analysis showing non-reversibility of the friction characteristics.

In the measurements, the following sensors were used.

1. Linear variable displacement transducer (LVDT) used for tracing the displacement of the main vibrating mass; it delivered voltage proportional to the position of the fixing point.
2. Linear velocity transducer (LVT) measuring velocity of the mass, relative to its end fixation points. Voltage appearing on its output was proportional to the velocity measured.
3. Two accelerometers measuring accelerations of the main mass and the support motion respectively, signals from the accelerometers were passed through a charge amplifier before being delivered to the data acquisition system.
4. FT mounted between main mass and the friction tongue delivered signal proportional to the force acting in the friction device (this signal also has been passed through a charge amplifier).
5. Pressure gauge mounted on the air supply valve (hose) for control of the clamping force.

The complete rig was mounted to the top of an electro-dynamic shaker. The base excitation provided by the shaker was controlled by a waveform generator or by the data acquisition and control system in the accompanying computer. Such type of rig assembly allowed for vibration around the resonance frequency of the system in the range of 5–25 Hz. Both under- and over-resonance regions were measured and used in the friction identification process.

Discrete time series of the data were obtained from the sensors and recorded using a data acquisition system. The system allowed also for controlling the input form of the signal feeding the shaker amplifier. This way an arbitrary wave could be used as system excitation. Such forms were used in the investigations because of the fact that other than multi-frequency periodic waves were much more useful in the identification of system properties than single ones.

3.2 Mathematical model

A simplified scheme of the experimental rig is shown in Fig. 5. The oscillator under consideration can be modelled as a one-degree-of-freedom mechanical oscillator to which a dry friction damper has been added. The dynamics of this system is described by the following second-order differential equation

$$M\ddot{y} = -2\,k[y - e(t)] - c[\dot{y} - \dot{e}(t)] - F_{\mathrm{f}} \tag{11}$$

where y, $\ddot{y}$, displacement (m), acceleration (m/s^2) of the mass; M, oscillating mass (with tongue) (kg); k, stiffness of springs (N/m); c, viscous damping coefficient (Ns/m); and $e(t)$, $\dot{e}(t)$, displacement (m), velocity (m/s) of the base, respectively.

The friction force F_{f} can be generally given in the form

$$F_{\mathrm{f}} = Nf(x, v)\mathrm{sgn}(v) \tag{12}$$

where N is normal pressure force and $f(x,v)$ denotes a function describing the friction characteristic. The subtractions $y - e(t)$ and $\dot{y} - \dot{e}(t)$ are relative displacement x and relative velocity v between the oscillating mass and the base, respectively. Thus, we can also determine the friction force F_{f} directly from equation (11) as follows

$$F_{\mathrm{f}} = -(M\ddot{y} + 2kx + cv) \tag{13}$$

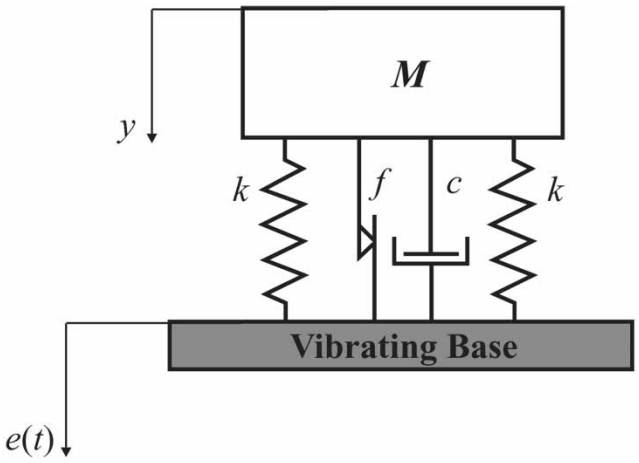

Fig. 5 The model of dry friction oscillator

3.3 Measurement of the friction force

Among researchers, there exist two schools of experimental measurement of friction force [**32**]:

(a) direct measurements using FT;
(b) indirect estimation by measuring motion signals and applying them to the equation governing the system dynamics.

In our experiment, direct measurement has been performed by means of an FT which is located between the main mass and the frictional tongue. However, the signal obtained from the FT does not completely reflect the actual friction force. This signal has been probably deformed by an influence of inertia force of unknown magnitude, which has its source in the mass of frictional tongue and/or main mass.

Therefore, we have determined the friction force indirectly on the basis of equation (13). According to equation (13), indirect estimation of friction force requires a knowledge of three signals and three parameters of the frictional system. The values of the relative displacement x and the relative velocity v have been delivered directly from LVDT and LVT transducers, respectively. The accelerometer connected to the main vibrating mass delivered the acceleration signal $\ddot{y}$. The main mass (with frictional tongue) of the oscillator amounts to $M = 3.35$ kg, total stiffness of springs is $2k = 5040$ N/m and the viscous damping coefficient applied in calculations was estimated as $c = 16.85$ Ns/m. This coefficient has been identified according to a method described in reference [**33**], which allows to separate Coulomb and viscous friction from free vibration decrements.

During the experiment, friction pads made from Teflon and constant air pressure of $p = 1$ bar in the clamping mechanism have been applied. Various forms of base excitation have been provided to the oscillator: harmonic, multi-periodic, and non-periodic.

3.4 Results

The results of the experiment, showing a relationship between the system attractor and friction characteristic, are presented in Figs 6 and 7. Each individual picture depicts the phase portrait of the system on the left and corresponding friction characteristic on the right. In the cases shown in Fig. 6, the friction oscillator has been excited by a harmonic signal of constant frequency η and amplitude A. The response of the system, visible in phase portraits, has a form of almost ellipsoidal loop, thus it is a limit cycle. Looking at Fig. 6, it is possible to compare the results obtained for various frequencies of forcing. A common feature of experimentally

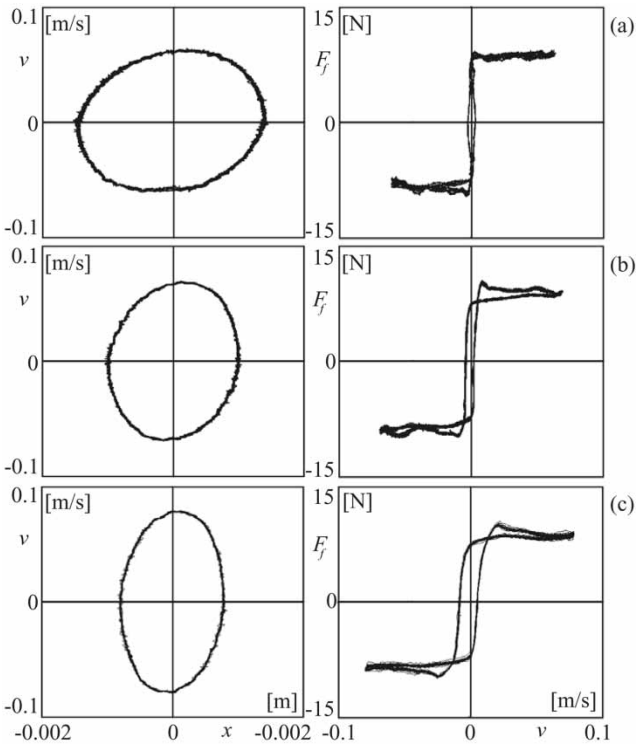

Fig. 6 Phase portraits and corresponding friction characteristics obtained experimentally during harmonic motion of the exciting base (shaker); $\eta = 5$ Hz, $A = 200$ mV (a), $\eta = 10$ Hz, $A = 100$ mV (b), $\eta = 15$ Hz, $A = 100$ mV (c)

generated friction characteristics from Fig. 6 is a clearly visible double hysteretic effect. The horizontal hysteresis is caused by the contact compliance during pre-sliding motion. The vertical hysteresis seems to be an effect of frictional memory. It is observed that during simple periodic motion, friction characteristics retain a regular hysteretic shape even if the size of the loop grows because of a change in the forcing parameters η and A.

Figure 7 illustrates the results of our experiment obtained during multi-periodic and non-periodic motion of the shaker. Such character of excitation leads to the multi-periodic (Figs 7(a) and (b)), quasi-periodic (Fig. 7(c)), and even chaotic (Fig. 7(d)) responses of the friction oscillator. The comparison of phase portraits with corresponding friction characteristics from Figs 7(a) to (d) shows that if the motion of the system becomes more complicated, then it is reflected on the friction characteristics.

4 NUMERICAL SIMULATION

4.1 Dry friction model

Taking under consideration the theoretical discussion and the experimental results presented earlier,

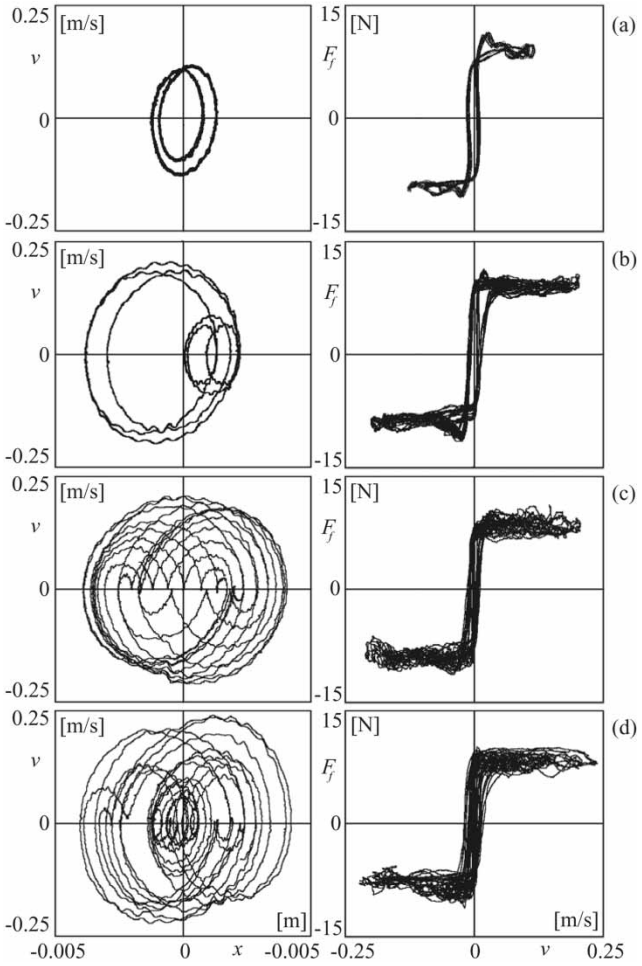

Fig. 7 Phase portraits and corresponding friction characteristics obtained experimentally during multi-periodic (a) and (b), quasi-periodic (c), and chaotic (d) response of the friction oscillator

the authors propose a novel dry friction model, which allows them to explain the observed frictional phenomena. The characteristic of the model, i.e. friction coefficient versus relative velocity, is depicted in Fig. 8. This approach can be treated as a developed version of the friction characteristic given by equation (10) with additionally modelled pre-sliding displacement. Its mathematical description is as follows

$$f(v)=\begin{cases} f_{\mathrm{st}}\mathrm{sgn}(v) & \text{for } f_{\mathrm{st}}<f_d \text{ and } \mathrm{sgn}\left(\dfrac{\mathrm{d}v}{\mathrm{d}t}v\right)>0 \\ f_{\mathrm{d}}\mathrm{sgn}(v) & \text{for } f_{\mathrm{st}}>f_d \text{ and } \mathrm{sgn}\left(\dfrac{\mathrm{d}v}{\mathrm{d}t}v\right)>0 \\ f_{\mathrm{d}}\mathrm{sgn}(v) & \text{for } \mathrm{sgn}\left(\dfrac{\mathrm{d}v}{\mathrm{d}t}v\right)<0 \end{cases} \tag{14}$$

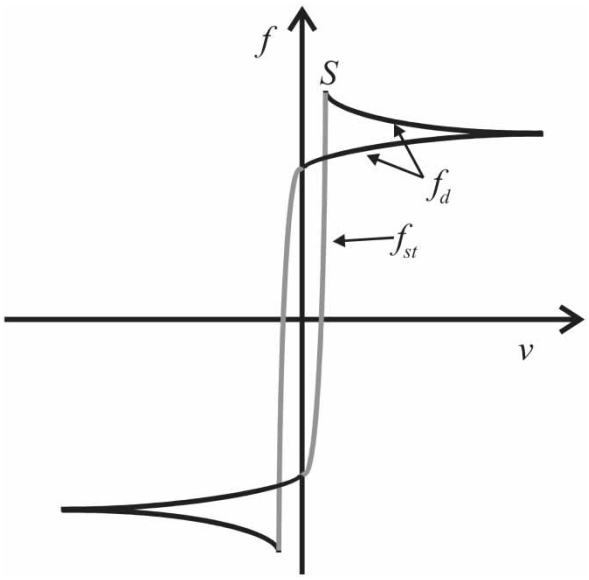

Fig. 8 Dry friction characteristic described by equations (14) to (16)

where

$$f_{\mathrm{st}}=\frac{1}{2}\frac{k_{\mathrm{s}}}{N}\frac{v^2}{|\mathrm{d}v/\mathrm{d}t|+\varepsilon}-(2f_{\mathrm{C}}-f_{\mathrm{S}}) \tag{15}$$

and

$$f_{\mathrm{d}}=f_{\mathrm{C}}\left[1+\frac{f_{\mathrm{S}}-f_{\mathrm{C}}}{f_{\mathrm{C}}}\exp\left(-d\frac{|v|}{|v-\tau(\mathrm{d}v/\mathrm{d}t)|+\delta}\right)\mathrm{sgn}\left(\frac{\mathrm{d}v}{\mathrm{d}t}v\right)\right] \tag{16}$$

Equation (15) describes the static friction coefficient during the compliant contact phase of motion (grey curves in Fig. 8). The friction force in stick phase is $F_{\mathrm{st}}=k_{\mathrm{s}}\ z$ and its time derivative is $\mathrm{d}F_{st}/\mathrm{d}t=k_{\mathrm{s}}\ \mathrm{d}z/\mathrm{d}t$, where k_{s} is the contact stiffness and z is an internal variable (Fig. 9). While sticking, the relative velocity of the frictional damper surfaces $w=\mathrm{d}x/\mathrm{d}t-\mathrm{d}z/\mathrm{d}t$ is equal to zero, hence $\mathrm{d}x/\mathrm{d}t=\mathrm{d}z/\mathrm{d}t$ and

$$\frac{\mathrm{d}F_{\mathrm{st}}}{\mathrm{d}t}=\frac{\mathrm{d}F_{\mathrm{st}}}{\mathrm{d}v}\frac{\mathrm{d}v}{\mathrm{d}t}=k_{\mathrm{s}}\frac{\mathrm{d}x}{\mathrm{d}t}\Rightarrow\frac{\mathrm{d}F_{\mathrm{st}}}{\mathrm{d}v}=k_{\mathrm{s}}\left(\frac{\mathrm{d}v}{\mathrm{d}t}\right)^{-1}v \tag{17}$$

Rearranging and integrating equation (17), they obtain

$$F_{\mathrm{st}}=\frac{1}{2}k_{\mathrm{s}}\left(\frac{\mathrm{d}v}{\mathrm{d}t}\right)^{-1}v^2-F_0 \tag{18}$$

where F_0 is an initial value of the force F_{st} for zero relative velocity $v=\mathrm{d}x/\mathrm{d}t$, thus $F_0=N[f_{\mathrm{C}}-(f_{\mathrm{S}}-f_{\mathrm{C}})]$.

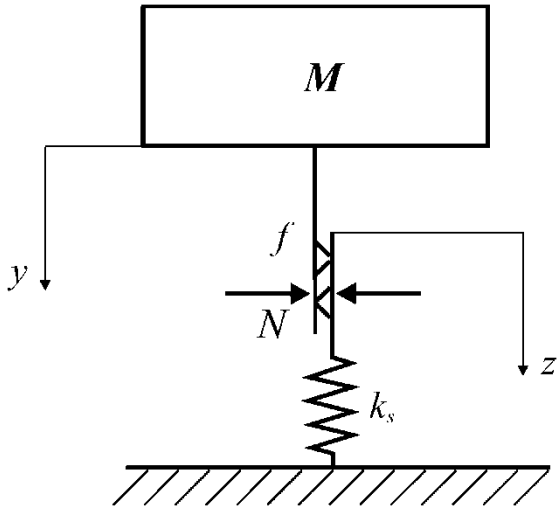

Fig. 9 The model of dry friction damper with the contact compliance

Equation (15) is obtained by substituting $F_{st} = Nf_{st}$, where N is a pressure force.

Frictional memory during slip phase (black curves in Fig. 8) is modelled in equation (16) in two ways:

(a) by the non-reversibility caused by the signum function;
(b) by the time delay τ in relative velocity, because $v(t-\tau) \approx v(t) - \tau\, \mathrm{d}v/\mathrm{d}t$.

The Stribeck effect is connected with the exponential factor in equation (16). An intersection of f_{st} and f_d curves (point S in Fig. 8), where a transition from stick to slip takes place, causes varying break-away friction force. The numerical analysis carried out has shown that its dependence on the dwell time has a character similar to the function shown in Fig. 1(b). The small parameters ε (m/s^2) and δ (m/s) introduced in equations (15) and (16) avoid zero values of the denominators. These parameters are of 10^{-3} in magnitude and this value has been selected by running an extensive numerical simulation programme. Larger values of about 10^{-2} result in significant differences between equation (15) and original equation (18) for non-zero accelerations. Very small values of ε and δ can cause problems when the acceleration is close to zero.

From a viewpoint of practical application, the presented approach can be classified as a static, seven-parameter friction model consisting of three non-dimensional parameters p, f_S, f_C, contact stiffness k_s, time delay τ, and two small parameters mentioned earlier. In addition, the pressure force N appears in the description of stick phase. According to our classification introduced in section 2, the proposed model is sensitive to the system dynamics. This sensitivity is caused by an inclusion of the acceleration to the mathematical model, what is a result of pre-sliding displacement (equation (15)) or frictional lag (equation (16)). Summing up, our dry friction model allows us to simulate various frictional phenomena, i.e. contact compliance, frictional memory, non-reversibility, varying break-away force, and Stribeck effect.

4.2 Numerical analysis of dry friction oscillator

In the numerical analysis, the authors have applied friction characteristics given by equations (14) to (16) to the mathematical model of the experimental rig given by equation (11), which can be rewritten (for numerical simulations) in the form of two first-order differential equations

$$\begin{aligned} \dot{y}_1 &= y_2 \\ \dot{y}_2 &= -\frac{2k}{M} y_1 - \frac{c}{M} y_2 + \frac{E}{M}[e(t) + \dot{e}(t)] - \frac{N}{M} f(v) \end{aligned} \tag{19}$$

where $y_1 = y$, $y_2 = \dot{y}$, $v = y_2 - \dot{e}(t)$, N is a pressure force, and E, an amplitude of kinematic forcing. Similarly, as during lab experiment, various exciting functions have been applied in numerical simulations: harmonic, multi-periodic, and chaotic. The parameters of the oscillator have been taken from the experiment (section 3.3). In addition, the value of the pressure force $N = 25$ N and amplitude of excitation $E = 0.01$ m are assumed. The parameters of the friction model are as follows: $p = 30$, $f_S = 0.3$, $f_C = 0.25$, contact stiffness $k_s = 10^6$ N/m, time delay $\tau = 0.1$ s and small parameters $\varepsilon = 10^{-3}$ m/s^2, and $\delta = 10^{-3}$ m/s. The results of numerical experiment are demonstrated in Fig. 10, where phase portraits of the simulated oscillator, presenting various system responses, and corresponding forms of friction characteristic (equations (14) to (16)) are depicted. An analogous (like in experiment) relationship is observed between the shape of friction characteristic and the response of the friction oscillator.

5 REMARKS AND CONCLUSIONS

Theoretical and experimental analysis presented in this article demonstrated how complex is the problem of friction modelling. Experimental analysis presented in section 3 confirmed an existence of various phenomena accompanying dry friction processes, i.e. hysteretic effects caused by frictional memory or contact compliance, varying break-away force, and Stribeck effect. These friction accompanying phenomena can cause the 'mapping

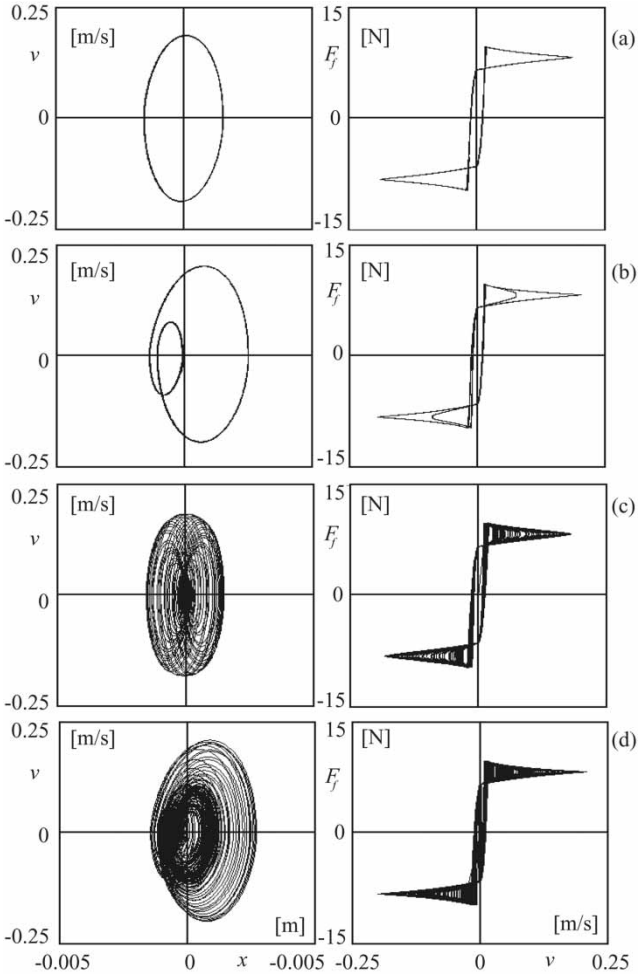

Fig. 10 Phase portraits and corresponding friction characteristics generated from numerical simulations of the friction oscillator (equation (19)) with friction model given by equations (14) to (16) for: harmonic (a) two-periodic (b), quasi-periodic (c), and chaotic (d) response of the friction oscillator

effect' described in section 2. In Figs 6 and 7, we can see that 'mapping effect' appears also in our dry friction oscillator. Regular friction hysteresis corresponds to regular, periodic motion (Fig. 6), and friction characteristics of complicated shape are connected with more complex system dynamics (Fig. 7). Hence, dynamical behaviour of friction force can be treated as a reflection of the system attractor. A problem is to recognize a strict rule governing such mapping. There appear the following questions – what influences the size of the frictional hysteresis? Whether these exists qualitative differences between friction characteristics during regular quasi-periodic motion (Fig. 8(c)) and irregular motion (Fig. 8(d))? Such differences between characteristics shown in Figs 7(c) and 7(d) are not visible. However, it does not mean that they do not exist. In order to find an answer for the above questions more detailed analysis of experimental data, using more advanced tools, e.g. Poincaré maps, dimensions of attractors, Lyapunov exponents reconstructed or estimated from experimental time series, is required. Such analysis are to be performed in the near future. It should be emphasized that the hysteresis of compliant contact (around the vertical axis of friction characteristic) observed in Figs 7 and 8 can only partly be accredited to the compliance of the clamping device.

A mechanism of mapping effect can be partly explained by theoretical analysis of friction models, presented in section 2. A brief review of several known, static and dynamic friction models was performed. Next, the authors introduced a division of these models into two categories: sensitive and insensitive to the system dynamics. Such criterion is strongly connected with our experimental observations. The authors classify as sensitive these friction models (static or dynamic), which can explain the mapping effect, i.e. they model the hysteretic effect of frictional memory at least. In Figs 6 and 7, a complexity of dry friction modelling is very well illustrated. It is observed that for the same friction oscillator both sensitive and insensitive friction models can be applied. For smaller frequencies of oscillation and relative velocities even the insensitive, classical Coulomb model (Fig. 7(a)) is sufficient to describe a friction force behaviour. However, if frequency and velocity increases, hysteretic effects become more and more visible (Figs 6(b) and 6(c)) leading to friction characteristics of complicated shape during more complex response of the friction oscillator (Figs 7(a) to (d)). In such cases, the sensitive friction models are required for more precise modelling of friction force dynamics.

On the basis of the analysis carried out on the dry friction oscillator, the authors have proposed in section 4.1, a new friction model accommodating our experimental observations and theoretical considerations. Advantages of this model are as follows:

(a) simplicity for application in numerical simulations – it is a static friction approach depending on seven parameters only;
(b) universality, i.e. the model can be easily reduced to the other known friction characteristics;
(c) it allows to simulate various frictional phenomena, i.e. contact compliance, frictional memory, non-reversibility, varying break-away force, and Stribeck effect.

In section 4.2, the numerical studies of the experimental friction oscillator modelled by equations (14) to (16), have been carried out. Comparisons of numerical (Figs 10(a) to (d)) and experimental results (Figs 6(a) to (c) and 7(a) to (d)) confirm that the

proposed dry friction model is a good approximation of the observed frictional phenomena.

ACKNOWLEDGEMENTS

This study has been supported by the Polish Department for Scientific Research (DBN) under project no. PB 0804/T07/2003/25 and the University of Aberdeen. The authors would like to thank the anonymous reviewers for the constructive comments.

REFERENCES

1 **Bell, R.** and **Burdekin, M.** A study of stick-slip motion of machine tool feed drives. *Proc. Instn Mech. Engrs*, 1970, **184**, 543–557.
2 **Den Hartog, J. P.** Forced vibrations with combined Coulomb and viscous friction. *Trans. ASME*, 1931, **53**, 107–115.
3 **Fenny, B. F.** and **Moon, F. C.** Chaos in a forced dry friction oscillator: experiment and numerical modelling. *J. Sound Vib.*, 1994, **170**(3), 303–323.
4 **Haessig, D. A.** and **Friedland, B.** On the modelling and simulation of friction. *J. Dyn. Systems Meas. Control Trans ASME*, 1991, **113**(3), 354–362.
5 **Harnoy, A.** and **Friedland, B.** Modeling and simulation of elastic and friction forces in lubricated bearings for precise motion control. *Wear*, 1994, **172**, 155–165.
6 **Hess, D. P.** and **Soom, A.** Friction at a lubricated line contact operating at oscillating sliding velocities. *J. Tribol.*, 1990, **112**, 147–152.
7 **Johannes, V. I., Green, M. A.,** and **Brockley, C. A.** The role of the rate of application of the tangential force in determining the static friction coefficient. *Wear*, 1973, **24**, 381–385.
8 **Liang, J.-W.** and **Feeny, B. F.** Dynamical friction behavior in a forced oscillator with a compliant contact. *J. Appl. Mech.*, 1998, **65**, 250–257.
9 **Olsson, H., Åström, K. J., Canudas de Wit, C., Gäfvert, M.,** and **Lischinsky, P.** Friction models and friction compensation. *Eur. J. Contr.*, 1998, **4**(3), 176–195.
10 **Popp, K.** and **Stelter, P.** Non-linear oscillations of structures induced by dry friction. In *Non-linear dynamics in engineering systems* (Ed. W. Schiehlen), 1990 (Springer, New York).
11 **Powell, J.** and **Wiercigroch, M.** Influence of non-reversible Coulomb characteristics on the response of a harmonically excited linear oscillator. *Mach. Vib.*, 1992, **1**(2), 94–104.
12 **Rabinowicz, E.** The nature of the static and kinetic coefficients of friction. *J. Appl. Phys.*, 1951, **22**(11), 1373–1379.
13 **Shaw, S. W.** On the dynamic response of a system with dry friction. *J. Sound Vib.*, 1986, **108**, 305–325.
14 **Stefański, A., Wojewoda, J.,** and **Wiercigroch, M.** Numerical analysis of duffing oscillator with dry friction. *Mech. Mech. Eng.*, 2000, **4**(2), 127–137.
15 **Stefański, A., Wojewoda, J., Wiercigroch, M.,** and **Kapitaniak, T.** Chaos caused by non-reversible dry friction. *Chaos, Solitons Fractals*, 2003, **16**, 661–664.
16 **Stefański, A., Wojewoda, J.,** and **Furmanik, K.** Experimental and numerical analysis of self – excited friction oscillator. *Chaos, Solitons Fractals*, 2001, **12**, 1691–1704.
17 **Stribeck, R.** Die wesentlichen Eigenschaften der Gleit- und Rollenlager – the key qualities of sliding and roller bearings. *Zeitschrift des Vereines Deutscher Ingenieure*, 1902, **46**(38,39), 1342–1348, 1432–1437.
18 **Tolstoi, D. M.** Significance of the normal degree of freedom and natural normal vibrations in contact friction. *Wear*, 1967, **10**, 199–213.
19 **Wiercigroch, M. A.** Note on the switch function for the stick-slip phenomenon. *J. Sound Vib.*, 1994, **175**, 700–705.
20 **Wiercigroch, M., Sin, V. W. T.,** and **Liew, Z. F. K.** Non-reversible dry friction oscillator: design and measurements. *Proc. Instn Mech. Engrs*, 1999, **213**(C), 527–534.
21 **Wiercigroch, M.** Comments on the study of a harmonically excited linear oscillator with a Coulomb damper. *J. Sound Vib.*, 1993, **167**(3), 560–563.
22 **Wojewoda, J., Kapitaniak, T., Barron, R.,** and **Brindley, J.** Complex behaviour of a quasiperiodically forced system with dry friction. *Chaos, Solitons Fractals*, 1993, **3**(1), 35–46.
23 **Wojewoda, J.** Chaotic behavior of friction force. *Int. J. Bifurcation Chaos*, 1992, **2**(1), 205–209.
24 **Courtney-Pratt, J. S.** and **Eisner, E.** The effect of a tangential force on the contact of metallic bodies. *Proc. Royal Soc.*, 1956, **A238**, 529–550.
25 **Coulomb, C. A.** Théorie des machines simples, *Mémoires de Mathématique et de Physique de l'Academie des Sciences*, 1785, **10**, 161–331.
26 **Babakov, I. M.** *Theory of vibrations* (in Russian), 1968 (Nauka, Moscow).
27 **Armstrong-Hélouvry, B., Dupont, P.,** and **Canudas de Wit, C.** A survey of models, analysis tools and compensation methods for the control of machines with friction. *Automatica*, 1994, **30**(7), 1083–1138.
28 **Dahl, P.** A solid friction model. Technical report TOR-0158(3107–18)-1, The Aerospace Corporation, El Segundo, CA, 1968.
29 **Ramberg, W.** and **Osgood, W. R.** Description of stress-strain curves by three parameters. Technical note 902, National Advisory Committee for Aeronautics, Washington, 1943.
30 **Bliman, P.-A.** and **Sorine, M.** Easy-to-use realistic dry friction models for automatic control. In Proceedings of 3rd European Control Conference, Rome, Italy, 1995, pp. 3788–3794.
31 **Canudas de Wit, C., Olsson, H., Åström, K. J.,** and **Lischinsky, P.** A new model for control of systems with friction. *IEEE Trans. Automat. Contr.*, 1995, **40**(3), 419–425.
32 **Liang, J.-W.** and **Feeny, B. F.** A comparison between direct and indirect friction measurements in a forced oscillator. *J. Appl. Mech.*, 1998, **65**, 783–786.
33 **Liang, J.-W.** and **Feeny, B. F.** Identifying Coulomb and viscous friction from free-vibration decrements. *Nonlinear Dynam.*, 1998, **16**, 337–347.

APPENDIX

Notation

a_1, a_2	constants controlling a modified non-reversible friction model, equation (10)
a, b	constants controlling the original non-reversible friction model, equation (3)
A	amplitude of excitation (mV)
c	viscous damping coefficient
d	constant controlling a modified non-reversible friction model, equation (16)
$e(t)$	displacement of the base
$\dot{e}(t)$	velocity of the base
E	amplitude of excitation (m)
$f(x, v)$	function describing the friction
f_C	coefficient of Coulomb friction
f_S	coefficient of static friction
f_{st}, f_d	branches of friction characteristics
$f_u(v)$, $f_l(v)$	upper and lower parts of the characteristic
F_C	Coulomb friction value
F_f	friction force
$F_S(\gamma, t_d)$	describes the varying friction level at break-away
F_{st}	friction force in the stick phase
F_0	initial value of the force F_{st} for zero relative velocity
k	stiffness of springs
k_s	contact stiffness
M	oscillating mass (with tongue)
N	normal pressure force
p	air pressure
t_d	dwell time
v	relative velocity
v_S	Stribeck velocity
w	relative velocity of the frictional damper surfaces
x	relative displacement
y	coordinate of the mass motion
z	average bristle deflection
α	determines the shape of stress-strain curve
β	contact stiffness
γ	empirical parameter
δ	small parameter (m/s)
ε	small parameter (m/s^2)
η	frequency
η_1, η_2	constants controlling the dry and viscous friction in equation (2)
σ	the stiffness coefficient
σ_0, σ_1	determine the bristles stiffness and the bristles damping, respectively
τ	time delay